International Journal of Mathematics and Physical Sciences Research ISSN 2348-5736 (Online)
Vol. 14, Issue 1, pp: (64-75), Month: April 2026 - September 2026, Available at: www.researchpublish.com

Hyperbolic Reconstruction of an Anisotropic Bianchi Type-I Cosmology with a Cubic Dark Energy Fluid

M. M. Sancheti[1], S. S. Wankhede[2]*

[1,2]Department of Mathematics, R.A. College, Washim-445550, India

DOI: https://doi.org/10.5281/zenodo.20728967

Published Date: 17-June-2026

Abstract: **We investigate an anisotropic Bianchi type I cosmological model in General Relativity, employing a nonlinear cubic equation of state $p = \lambda\rho^3 + \mu\rho^2 - \rho$ together with a hyperbolic Hubble flow parametrization $H(t) = \alpha\tanh(\beta t)$. Exact analytical expressions are obtained for the scale factor, directional scale factors, Hubble parameter, deceleration, jerk and statefinder parameters, energy density, an effective pressure and equation of state, expansion and shear scalars, the anisotropy ratio σ^2/θ^2, a sound-speed (stability) parameter, the null and strong energy conditions, the $Om(z)$ diagnostic, and – derived directly and independently of λ, μ from the field equations – the true anisotropic skewness parameters $\gamma(t)$ and $\delta(t)$.**

The model is *exactly isotropic at* $t = 0$ ($\sigma^2 = 0$); γ and δ are formally singular there only because the normalizing energy density ρ vanishes, while the underlying anisotropic stresses remain finite. As cosmic time increases, σ^2, γ, and δ all relax toward small, non-zero constants, so the universe evolves toward a state of permanent, bounded ("frozen") anisotropy rather than isotropizing – a result stated sharply via the exactly constant anisotropy ratio $\sigma^2/\theta^2 \approx 1.11 \times 10^{-3}$, which depends only on the anisotropy exponents m, n. The deceleration parameter satisfies $q(t) < -1$ for all $t > 0$ (kinematic super-acceleration, $\dot{H} > 0$, despite $\omega(t) \geq -1$), diverging as $t \to 0^+$ and approaching the de Sitter value $q = -1$ only as $t \to \infty$; the corresponding jerk parameter $j(t)$ and statefinder pair (r, s) approach the ΛCDM fixed point $(r, s) = (1, 0)$ from the quintessence-like quadrant as $t \to \infty$.

For the adopted parameters ($\lambda = 0.02$, $\mu = 0.1$, chosen to satisfy the causality bound $3\lambda\rho_\infty^2 + 2\mu\rho_\infty \leq 2$), the effective equation-of-state parameter $\omega(t)$ interpolates monotonically from the de Sitter value $\omega = -1$ at $t = 0$ to a mild quintessence value $\omega \approx -0.20$ at late times, the null energy condition holds throughout, the strong energy condition is violated only in a brief early window ($t \lesssim 2.1$) and is restored thereafter, and the sound speed satisfies $c_s^2 \leq 1$ for all t. Phantom behaviour ($\omega < -1$) is not realized for $\lambda, \mu > 0$ and would require $\lambda < 0$ or $\mu < 0$.

The model thus provides a causally consistent, exactly solvable framework for an anisotropic universe that begins isotropic, passes through a transient dark-energy-like phase, and settles into a permanently and mildly anisotropic, quintessence-dominated late-time state.

Keywords: **Bianchi type I cosmology; Anisotropic dark energy; Cubic equation of state; Exact solutions; State finder and Om(z) diagnostics; Quintessence.**

1. INTRODUCTION

The discovery of the accelerated expansion of the universe through observations of Type Ia supernovae marked one of the most important breakthroughs in modern cosmology and established the existence of dark energy as a dominant constituent of the universe [1, 2]. Subsequent observations involving the cosmic microwave background, baryon acoustic oscillations, galaxy redshift surveys, and large-scale structure further confirmed that the present universe is undergoing accelerated expansion [16, 14, 15, 17]. The standard cosmological model, based on General Relativity and a cosmological constant, successfully explains many observational properties of the universe; several theoretical issues, including the cosmological constant problem, the coincidence problem, and the physical nature of dark energy, nevertheless remain open [5, 6, 7, 18].

The homogeneous and isotropic Friedmann–Robertson–Walker models successfully describe the large-scale dynamics of the universe [11, 12, 13]. However, anisotropic effects may have played a role during early cosmic epochs, motivating the study of anisotropic cosmologies. Among these, the Bianchi type I universe is one of the simplest and most widely studied generalizations of the FRW universe [4, 24], allowing independent expansion rates along three spatial directions while preserving spatial homogeneity [21, 22, 23].

A second important ingredient is the choice of equation of state for the cosmic fluid. Linear barotropic equations of state are often insufficient to capture rich dark energy dynamics; nonlinear equations of state Chaplygin gas, logarithmic, polytropic, quadratic, and cubic forms have therefore attracted considerable attention [8, 9, 10, 20]. Motivated by recent investigations of anisotropic cosmological models with quadratic equations of state in both General Relativity and modified gravity, which demonstrated that nonlinear equations of state can describe accelerating cosmological evolution together with anisotropic dark-energy behaviour [26], we consider here the nonlinear cubic equation of state

$$p = \lambda\rho^3 + \mu\rho^2 - \rho, \tag{1}$$

where λ and μ are constants governing the nonlinear cosmic fluid dynamics.

A third ingredient is the choice of Hubble parametrization. Suitable parametrizations provide exact analytical reconstructions of cosmological evolution and describe smooth transitions between cosmic phases [19, 25]. We adopt the hyperbolic Hubble flow

$$H(t) = \alpha\tanh(\beta t), \qquad \alpha, \beta > 0, \tag{2}$$

which is finite throughout cosmic evolution and asymptotically approaches a constant, generating de Sitter-type behaviour at late times.

The paper is organized as follows. **Section 2** presents the field equations for the anisotropic Bianchi type I metric. **Section 3** obtains the exact solution using a power-law anisotropy ansatz, Eq. (1), and Eq. (2). **Section 4** discusses the physical and kinematical quantities, including the energy conditions, sound speed, shear scalar, and the anisotropic skewness parameters. **Section 5** summarizes the conclusions.

2. METRIC AND FIELD EQUATIONS

We consider the Bianchi type I metric

$$ds^2 = -dt^2 + A^2(t)\,dx^2 + B^2(t)\,dy^2 + C^2(t)\,dz^2. \tag{3}$$

The Einstein field equations are $R_{ij} - 1/2\,Rg_{ij} = T_{ij}$. We take an anisotropic fluid energy–momentum tensor

$$T^i_j = \mathrm{diag}[-\rho,\ \omega\rho,\ (\omega+\gamma)\rho,\ (\omega+\delta)\rho], \tag{4}$$

where ω is the (direction-free) equation-of-state parameter and γ, δ are skewness parameters describing pressure anisotropy along the y- and z-directions relative to the x-direction. With $H_A \equiv \dot{A}/A$, $H_B \equiv \dot{B}/B$, $H_C \equiv \dot{C}/C$, the field equations reduce to

$$H_AH_B + H_BH_C + H_CH_A = \rho, \tag{5}$$

$$\frac{\ddot{B}}{B} + \frac{\ddot{C}}{C} + H_BH_C = -\omega\rho, \tag{6}$$

$$\frac{\ddot{A}}{A} + \frac{\ddot{C}}{C} + H_AH_C = -(\omega+\gamma)\rho, \tag{7}$$

$$\frac{\ddot{A}}{A} + \frac{\ddot{B}}{B} + H_AH_B = -(\omega+\delta)\rho. \tag{8}$$

The conservation equation, obtained from $\dot{\rho} + \sum_i H_i(\rho + p_i) = 0$ with $p_x = \omega\rho$, $p_y = (\omega+\gamma)\rho$, $p_z = (\omega+\delta)\rho$ and $H_A + H_B + H_C = 3H$, is

$$\dot{\rho} + 3H(1+\omega)\rho + \gamma\rho H_B + \delta\rho H_C = 0, \tag{9}$$

where H_B and H_C are the directional Hubble rates of the B- and C-directions (this corrects a mis-typeset version of this equation found in earlier drafts, in which H_B, H_C appeared as powers H^2, H^3 of the average Hubble parameter; Eq. (9) is dimensionally consistent and is not needed in the solution procedure below, but is retained for completeness).

The spatial volume and average scale factor are $V = ABC = a^3$, $a = (ABC)^{1/3}$, with

$$H = \frac{\dot{a}}{a}, \qquad q = -\frac{a\ddot{a}}{\dot{a}^2}, \qquad \theta = 3H, \qquad \sigma^2 = \frac{1}{2}\left(\sum_{i=1}^{3} H_i^2 - 3H^2\right). \tag{10}$$

3. SOLUTION OF THE FIELD EQUATIONS

Equations (5)–(8) are four equations for the seven unknowns $A, B, C, p, \rho, \gamma, \delta$ (with $\omega \equiv p/\rho$ once p, ρ are specified). To obtain a determinate solution we impose:

1. Power-law anisotropy: $A = B^m$, $C = B^n$, with m, n constant.
2. The cubic equation of state (1).
3. The hyperbolic Hubble parametrization (2).

From (2), $H = \dot{a}/a$ integrates to

$$a(t) = a_0 \cosh^{\alpha/\beta}(\beta t). \tag{11}$$

Since $V = ABC = B^{m+n+1} = a^3$,

$$A(t) = a_0^{\frac{3m}{m+n+1}} \cosh^{\frac{3m\alpha}{\beta(m+n+1)}}(\beta t), \tag{12}$$

$$B(t) = a_0^{\frac{3}{m+n+1}} \cosh^{\frac{3\alpha}{\beta(m+n+1)}}(\beta t), \tag{13}$$

$$C(t) = a_0^{\frac{3n}{m+n+1}} \cosh^{\frac{3n\alpha}{\beta(m+n+1)}}(\beta t). \tag{14}$$

It is convenient to define

$$h(t) \equiv \frac{\dot{B}}{B} = \frac{3\alpha}{m+n+1}\tanh(\beta t), \qquad H_A = mh, \quad H_B = h, \quad H_C = nh. \tag{15}$$

Substituting into Eq. (5) gives the energy density

$$\rho(t) = \frac{9\alpha^2(m+n+mn)}{(m+n+1)^2}\tanh^2(\beta t). \tag{16}$$

Using Eq. (1), the effective pressure and equation-of-state parameter are

$$p(t) = \lambda\rho(t)^3 + \mu\rho(t)^2 - \rho(t), \tag{17}$$

$$\omega(t) \equiv \frac{p(t)}{\rho(t)} = \lambda\rho(t)^2 + \mu\rho(t) - 1. \tag{18}$$

Equations (17)–(18) define an *effective*, isotropic-equivalent pressure and equation-of-state parameter via the cubic relation (1), used below to probe the bulk thermodynamic behaviour (energy conditions, sound speed) of the cosmic medium. The *true* directional pressure deviations $\gamma(t), \delta(t)$ appearing in (4) are obtained independently, directly from Eqs. (6)–(8), in Appendix A; they depend only on α, β, m, n and not on λ, μ.

4. PHYSICAL AND KINEMATICAL QUANTITIES

Throughout this section we illustrate the analytical results with the parameter set

$$\alpha = 1.2, \quad \beta = 0.8, \quad m = 1.1, \quad n = 0.9, \quad \lambda = 0.02, \quad \mu = 0.1, \quad a_0 = 1. \tag{19}$$

The value of μ is reduced relative to a naive choice ($\mu = 0.5$) specifically so that the causality bound derived in §4.2 is satisfied; see the remark there.

4.1 Scale Factor, Hubble Parameter, and Deceleration Parameter

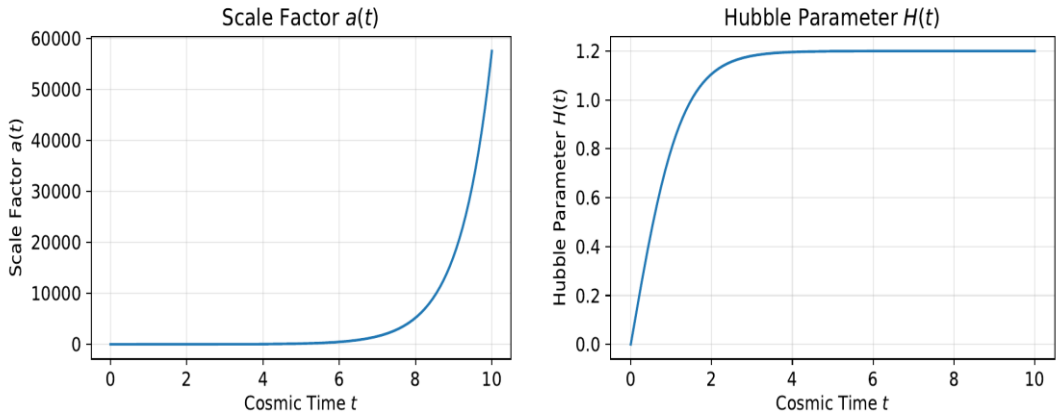

Fig.1: Evolution of the scale factor $a(t)$ (left) and Hubble parameter $H(t)$ (right) for the parameters (19).

The scale factor (11) increases smoothly and without bound (Fig. 1, left), with no curvature singularity at any finite t. The Hubble parameter (2) is positive for all $t > 0$ and approaches the constant value α at late times (Fig. 1, right), corresponding to de Sitter-type expansion.

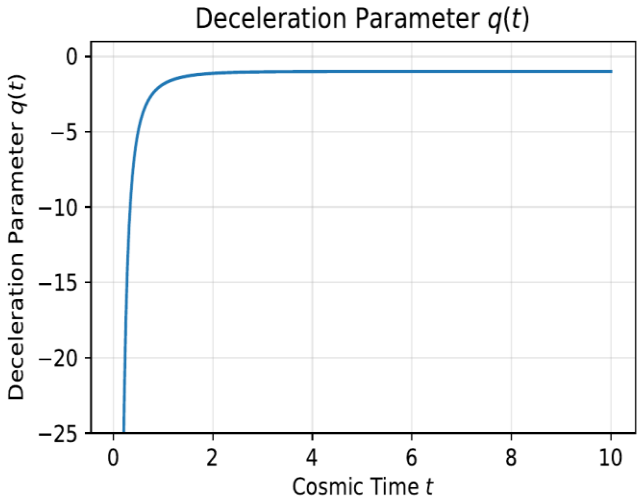

Fig.2: Deceleration parameter $q(t)$, satisfying $q(t) < -1$ for all $t > 0$ (kinematic super-acceleration) and approaching the de Sitter value $q = -1$ as $t \to \infty$. Note the divergence to $-\infty$ as $t \to 0^+$: the model does not describe an earlier decelerating epoch.

Using (10) and (11), the deceleration parameter is

$$q(t) = -1 - \frac{\beta \operatorname{sech}^2(\beta t)}{\alpha \tanh^2(\beta t)}. \qquad (20)$$

Since the second term is strictly positive for all $t > 0$, $q(t) < -1$ for *every* $t > 0$ (Fig. 2) – the model is not merely accelerating ($q < 0$) but *kinematically super-accelerating* ($\dot{H} > 0$) at every epoch, approaching the de Sitter value $q = -1$ only as $t \to \infty$. As $t \to 0^+$, $q \to -\infty$: the model has *no early decelerating (matter/radiation-dominated) phase* and should be understood as describing a late-time/dark-energy-era reconstruction rather than a complete cosmic history. (The relation between this kinematic super-acceleration and the thermodynamic equation-of-state parameter $\omega(t) \geq -1$ of §4.2 is discussed in §4.6.)

4.2 Energy Density, Effective Pressure, Equation of State, and Sound Speed

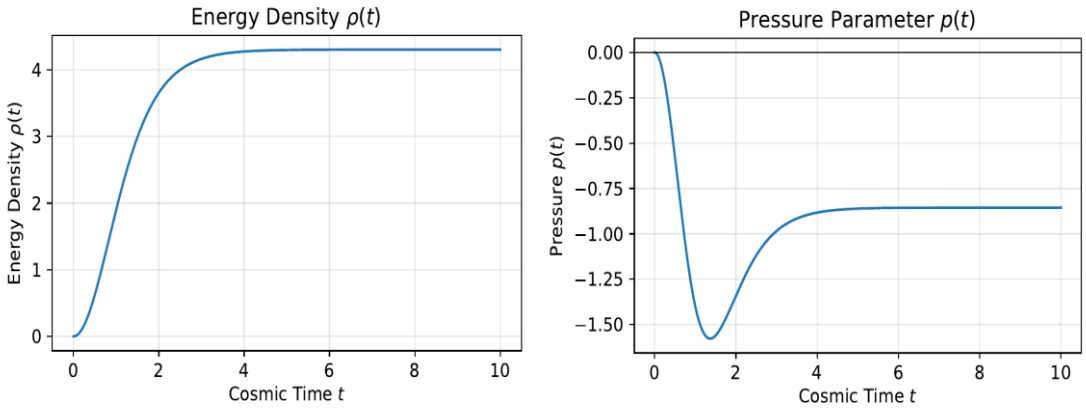

Fig.3: Energy density $\rho(t)$ (left, Eq. (16)) and effective pressure $p(t)$ (right, Eq. (17)) for the parameters (19).

The energy density (16) vanishes at $t = 0$ and increases monotonically to a finite asymptotic value

$$\rho_\infty = \frac{9\alpha^2(m+n+mn)}{(m+n+1)^2} \approx 4.306 \qquad (21)$$

(Fig. 3, left), with no singularity at any finite t. The effective pressure (17) vanishes at $t = 0$, becomes negative, reaches a minimum $p \approx -1.58$ near $t \approx 1.4$, and relaxes to $p_\infty \approx -0.86$ as $t \to \infty$ (Fig. 3, right): the effective pressure is negative throughout $t > 0$, consistent with accelerated expansion, and never enters the positive (stiff) regime for these parameters.

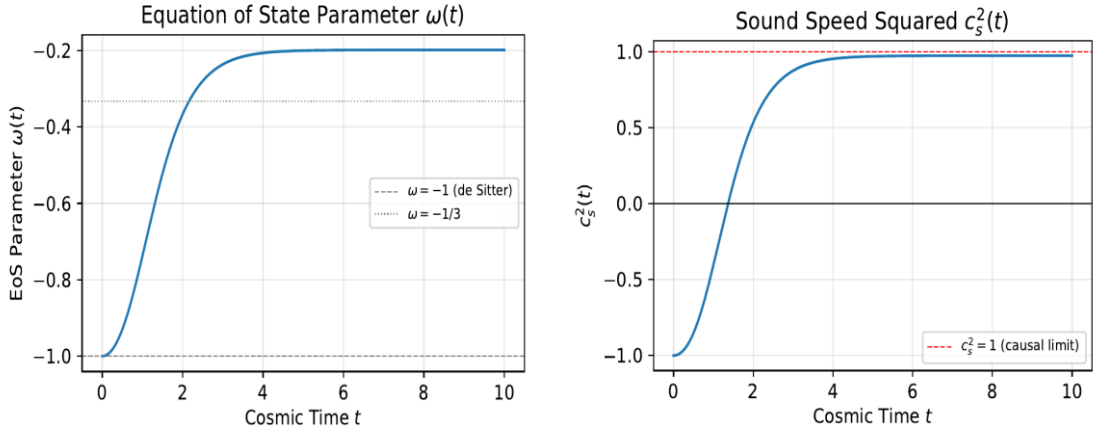

Fig.4: Effective equation-of-state parameter $\omega(t)$ (left, Eq. (18)) and sound speed squared $c_s^2(t)$ (right, Eq. (23)). The dashed/dotted reference lines mark $\omega = -1$ (de Sitter), $\omega = -1/3$, and the causal limit $c_s^2 = 1$.

The equation-of-state parameter (18) satisfies $\omega(0) = -1$ (the de Sitter / cosmological-constant boundary) and, since $d\omega/d\rho = 2\lambda\rho + \mu > 0$ for $\lambda, \mu > 0$, increases monotonically toward

$$\omega_\infty = \lambda\rho_\infty^2 + \mu\rho_\infty - 1 \approx -0.199. \qquad (22)$$

Thus $\omega(t) \in [-1, -0.199]$ for all $t \geq 0$ (Fig. 4, left): the model interpolates between a de Sitter-like phase at $t = 0$ and a mild quintessence-like phase at late times, *never reaching $\omega = -1/3$ from below in a way that would halt acceleration* – the acceleration itself is driven by the prescribed $H(t)$, while $\omega(t)$ characterizes the effective fluid's thermodynamics.

Since $\lambda\rho^2 + \mu\rho \geq 0$ for $\rho \geq 0$, $\lambda, \mu > 0$, we have $\omega(t) \geq -1$ for all t, with equality only at $t = 0$. **Phantom behaviour** ($\omega < -1$) would require $\lambda < 0$ or $\mu < 0$, and is not realized for the parameters (19).

The sound-speed parameter is

$$c_s^2(t) = \frac{dp}{d\rho} = 3\lambda\rho(t)^2 + 2\mu\rho(t) - 1. \quad (23)$$

$c_s^2(0) = -1$ (classically unstable near $t = 0$), c_s^2 increases monotonically, crosses zero near $t \approx 1.4$, and approaches

$$c_s^2(\infty) = 3\lambda\rho_\infty^2 + 2\mu\rho_\infty - 1 \approx 0.973. \quad (24)$$

From Fig. 4, right it is clear that, for all t, $c_s^2(t) \leq 1$: the effective fluid description is causal throughout. A value $c_s^2 > 1$ would signal superluminal sound propagation and a breakdown of causality in the effective fluid description. Requiring $c_s^2(\infty) \leq 1$ gives the bound

$$3\lambda\rho_\infty^2 + 2\mu\rho_\infty \leq 2\,. \quad (25)$$

For $\rho_\infty \approx 4.306$ and $\lambda = 0.02$, Eq. (25) requires $\mu \lesssim 0.103$; we adopt $\mu = 0.1$, which satisfies the bound ($3\lambda\rho_\infty^2 + 2\mu\rho_\infty \approx 1.97 < 2$). A larger value such as $\mu = 0.5$ would give $c_s^2(\infty) \approx 4.4 > 1$, i.e. an acausal late-time effective fluid, and should be avoided.

4.3 Energy Conditions

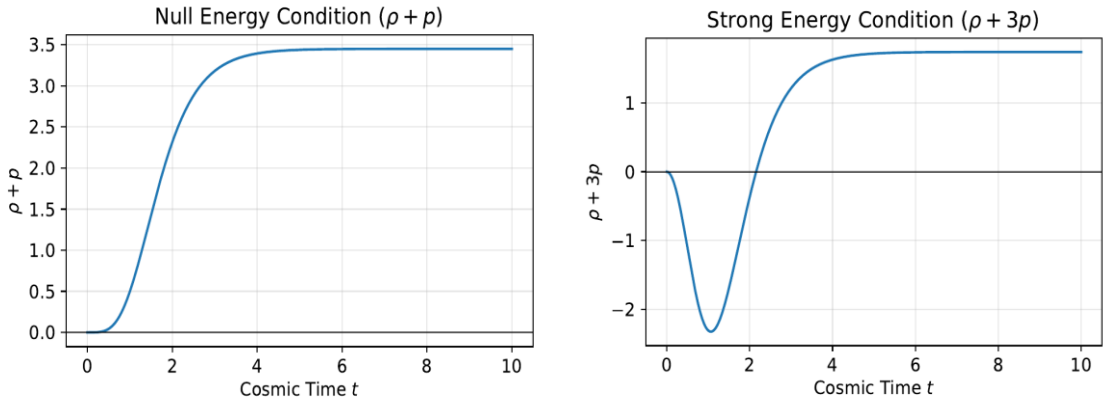

Fig.5: Null energy condition $\rho + p$ (left) and strong energy condition $\rho + 3p$ (right).

From (16)–(17),

$$\rho + p = \lambda\rho^3 + \mu\rho^2 = \rho^2(\lambda\rho + \mu) \geq 0. \quad (26)$$

for $\rho \geq 0$, $\lambda, \mu > 0$: the null energy condition (NEC) is satisfied for all t (Fig. 5, left), increasing monotonically from 0 to $\rho_\infty^2(\lambda\rho_\infty + \mu) \approx 3.45$.

The strong energy condition is governed by

$$\rho + 3p = \rho(3\lambda\rho^2 + 3\mu\rho - 2). \quad (27)$$

Since $\rho + 3p = 0$ at $t = 0$ and at $\rho = \rho_c$, the positive root of $3\lambda\rho^2 + 3\mu\rho - 2 = 0$; for the parameters (19), $\rho_c \approx 3.79$, corresponding to $t \approx 2.1$. For $0 < t \lesssim 2.1$, $\rho + 3p < 0$ and the strong energy condition (SEC) is violated; for $t \gtrsim 2.1$, $\rho + 3p > 0$ and the SEC is **restored**, approaching $\rho_\infty(1 + 3\omega_\infty) \approx 1.74$ as $t \to \infty$ (Fig. 5, right). The brief SEC-violating window near $t = 0$ corresponds to the transient dark-energy-like ($\omega \approx -1$) phase, while the late-time, SEC-satisfying regime corresponds to the mild quintessence phase ($\omega_\infty \approx -0.199$).

4.4 Expansion and Shear Scalar

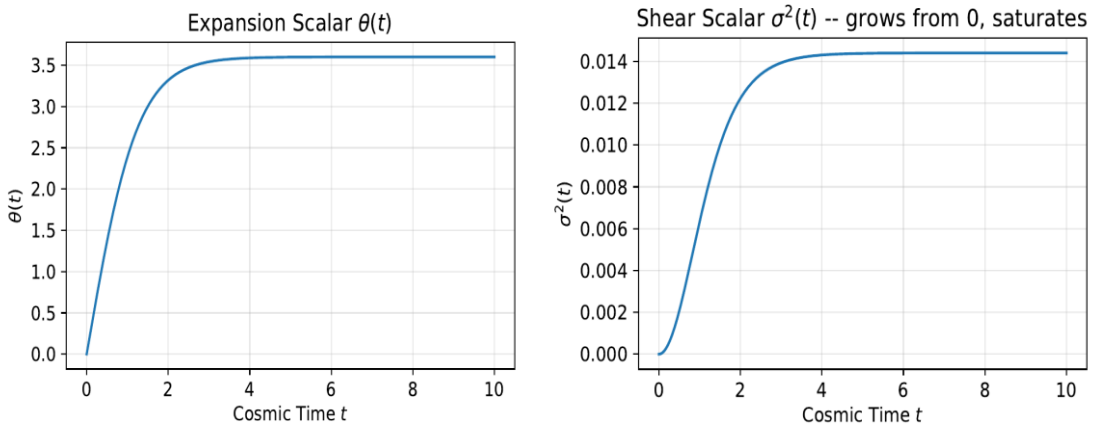

Fig.6: Expansion scalar $\theta(t) = 3H(t)$ (left) and shear scalar $\sigma^2(t)$ (right). Both increase monotonically from 0 and saturate at finite constants.

The expansion scalar is $\theta(t) = 3\alpha\tanh(\beta t)$, increasing monotonically from 0 to 3α (Fig. 6, left). The shear scalar, from (10) and (15), is

$$\sigma^2(t) = \frac{3\alpha^2(m^2+n^2+1-mn-m-n)}{(m+n+1)^2}\tanh^2(\beta t). \quad (28)$$

Using the identity $m^2 + n^2 + 1 - mn - m - n = 1/2\,[(m-n)^2 + (m-1)^2 + (n-1)^2] \geq 0$ (with equality only for $m = n = 1$, the isotropic FRW limit), $\sigma^2(t)$ is non-negative and increases monotonically from $\sigma^2(0) = 0$ to the finite constant

$$\sigma_\infty^2 = \frac{3\alpha^2(m^2+n^2+1-mn-m-n)}{(m+n+1)^2} \approx 0.0144\,. \quad (29)$$

From Fig. 6, right it is observed that**,** the model is *exactly isotropic at* $t = 0$. As $\theta(t)$ also approaches a constant (3α) at late times, the ratio σ^2/θ^2 approaches the non-zero constant $\sigma_\infty^2/(9\alpha^2)$: this is the opposite of isotropization in the usual sense (which requires $\sigma^2/\theta^2 \to 0$). Instead, the universe evolves from perfect isotropy toward a state of permanent, bounded (frozen) anisotropy, whose magnitude σ_∞^2 is controlled by how far m, n are from unity and vanishes identically in the isotropic limit $m = n = 1$.

Anisotropy ratio σ^2/θ^2

The frozen-anisotropy result can be stated even more sharply. Since $\sigma^2(t) \propto \tanh^2(\beta t)$ (Eq. (28)) and $\theta(t)^2 = 9\alpha^2\tanh^2(\beta t)$ share identical time-dependence, the ratio is *exactly constant for all* $t > 0$ (and extends continuously to $t = 0$ by continuity, since both vanish there at the same rate):

$$\frac{\sigma^2(t)}{\theta(t)^2} = \frac{m^2+n^2+1-mn-m-n}{3(m+n+1)^2} \equiv \text{const.} \quad (30)$$

Remarkably, this constant depends *only on* m, n – not on α, β, λ, or μ. For the adopted parameters, $\sigma^2/\theta^2 \approx 0.00111 = 1/900$ (Fig. 7 below). This is a stronger statement than "σ^2 approaches a constant": the anisotropy-to-expansion ratio is *conserved throughout the entire cosmic evolution*, not merely asymptotically – the clearest possible demonstration of frozen, rather than decaying, anisotropy.

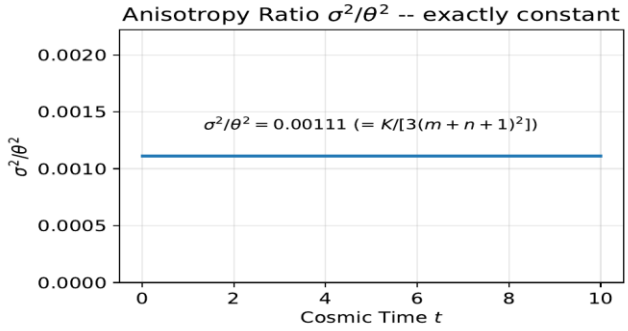

Fig. 7: Anisotropy ratio $\sigma^2(t)/\theta(t)^2$, exactly constant for all t (Eq. (30)).

4.5 Skewness Parameters

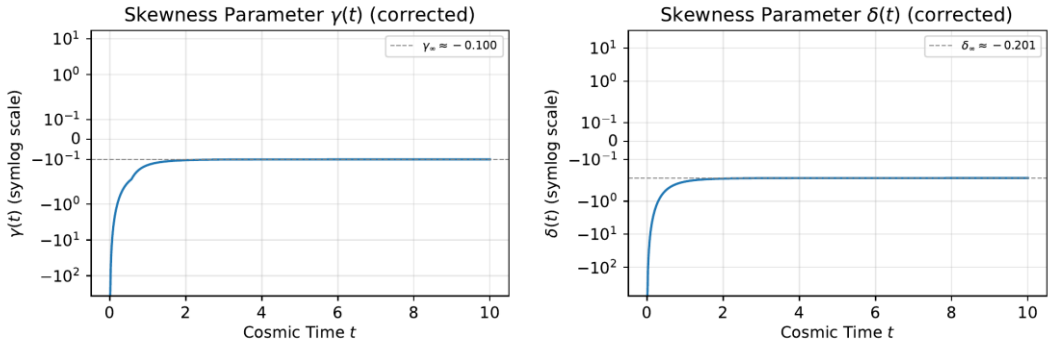

Fig. 8: Skewness parameters $\gamma(t)$ (left) and $\delta(t)$ (right), plotted on a symmetric-log vertical axis to display both the early divergence (a removable singularity caused by $\rho(t) \to 0$, not by a divergent anisotropic stress; see Appendix A) and the late-time plateaus $\gamma_\infty \approx -0.100$, $\delta_\infty \approx -0.201$.

The skewness parameters $\gamma(t)$ and $\delta(t)$, representing the directional pressure deviations $p_y - p_x = \gamma\rho$ and $p_z - p_x = \delta\rho$, are derived directly from Eqs. (6)–(8) in Appendix A:

$$\gamma(t) = -(m-1)\frac{\dot{h}(t) + (m+n+1)h(t)^2}{\rho(t)}, \tag{31}$$

$$\delta(t) = -(m-n)\frac{\dot{h}(t) + (m+n+1)h(t)^2}{\rho(t)}. \tag{32}$$

Crucially, $\gamma(t)$ and $\delta(t)$ depend only on α, β, m, n – they are independent of λ, μ – reflecting their purely geometric/kinematic origin. Because $\dot{h}(0) \neq 0$ while $\rho(0) = 0$, both functions diverge as $t \to 0^+$ (Fig. 8); however, the *numerators* $\gamma\rho|_{t=0} = -(m-1)\dot{h}(0)$ and $\delta\rho|_{t=0} = -(m-n)\dot{h}(0)$ – the actual anisotropic pressure differences – are finite. The divergence of γ, δ at $t = 0$ is therefore a normalization artefact (division by $\rho \to 0$), not a curvature singularity; the metric, ρ, p, θ, and σ^2 are all regular at $t = 0$.

As $t \to \infty$,

$$\gamma_\infty = -\frac{(m-1)(m+n+1)}{m+n+mn} \approx -0.100, \qquad \delta_\infty = -\frac{(m-n)(m+n+1)}{m+n+mn} \approx -0.201. \tag{33}$$

These small, non-zero, permanent values are consistent with the frozen, non-vanishing late-time shear of §4.4: the universe approaches, but never reaches, perfect isotropy in either its shear or its directional pressures.

4.6 Jerk Parameter and Statefinder Diagnostics

The jerk parameter $j = \dddot{a}/(aH^3)$ provides a third-order kinematic diagnostic beyond H and q. Using $\ddot{a}/a = \dot{H} + H^2$ and differentiating, $\dddot{a}/a = \ddot{H} + 3H\dot{H} + H^3$, so

$$j(t) = \frac{\dot{H}}{H^3} + 3\frac{\dot{H}}{H^2} + 1. \tag{34}$$

With $H = \alpha\tanh(\beta t)$, $\dot{H} = \alpha\beta\,\mathrm{sech}^2(\beta t)$, $\ddot{H} = -2\alpha\beta^2\tanh(\beta t)\,\mathrm{sech}^2(\beta t)$, and defining $k \equiv \beta/\alpha$ together with

$$X(t) \equiv \frac{\mathrm{sech}^2(\beta t)}{\tanh^2(\beta t)} = \mathrm{csch}^2(\beta t), \tag{35}$$

Eq. (20) becomes $q(t) = -1 - kX(t)$, and Eq. (34) reduces to the closed form

$$j(t) = 1 + k(3 - 2k)\,X(t) = 1 + k(3 - 2k)\,\mathrm{csch}^2(\beta t). \tag{36}$$

For the adopted parameters, $k = 2/3$ and $k(3 - 2k) = 10/9 > 0$, so $j(t) = 1 + 10/9\,\mathrm{csch}^2(\beta t) > 1$ for all $t > 0$, diverging as $t \to 0^+$ and decreasing monotonically to $j \to 1$ as $t \to \infty$ (Fig. 9).

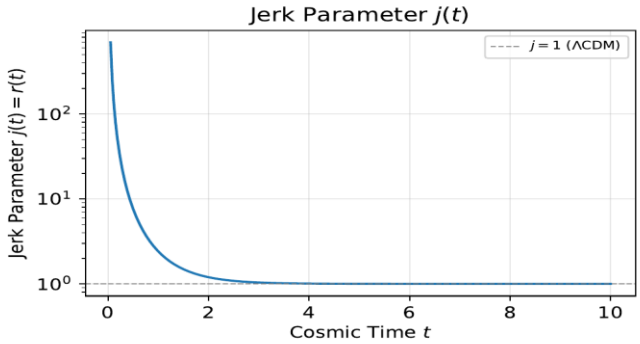

Fig. 9: Jerk parameter $j(t)$ (Eq. (36)), log scale, showing $j \to \infty$ as $t \to 0^+$ and $j \to 1$ (the ΛCDM value, dashed line) as $t \to \infty$.

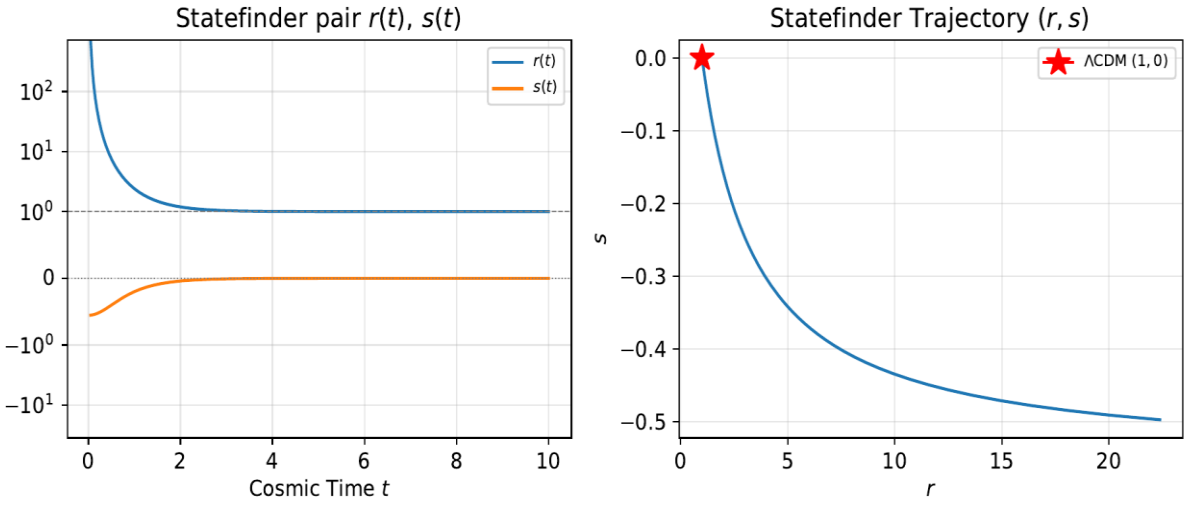

Fig. 10: Left: state finder pair $r(t), s(t)$ vs. cosmic time (symmetric-log vertical axis). Right: statefinder trajectory (r, s) (Eq. (37)), approaching the ΛCDM fixed point $(r, s) = (1, 0)$ (red star) from the region $s < 0$, $r > 1$ as $t \to \infty$.

The state finder pair (r, s) [27] is defined by $r \equiv j$ and $s \equiv (r - 1)/[3(q - 1/2)]$, for which ΛCDM corresponds identically to $(r, s) = (1,0)$. Substituting Eqs. (36) and $q = -1 - kX$,

$$s(t) = \frac{k(3-2k)X(t)}{3q(t)-3/2} = -\frac{k(3-2k)X(t)}{9/2+3kX(t)}. \tag{37}$$

As $t \to 0^+$ ($X \to \infty$), $s \to -(3 - 2k)/3 = -5/9 \approx -0.556$ and $r = j \to \infty$; as $t \to \infty$ ($X \to 0$), $(s, r) \to (0,1)$ – the model asymptotically approaches the ΛCDM statefinder point from the quadrant $s < 0$, $r > 1$ (Fig. 10), characteristic of quintessence-like (rather than Chaplygin-gas-like, $s > 0$) dark energy.

Kinematic vs. thermodynamic phantom divide: Since $X(t) > 0$ for all finite t, Eq. (20) gives $q(t) < -1$ for *all* t, approaching -1 only as $t \to \infty$: the model is kinematically "super-accelerated" ($\dot{H} > 0$, i.e. $q < -1$) at *every* epoch. This might naively suggest phantom behaviour, yet §4.2 showed $\omega(t) \geq -1$ (thermodynamically non-phantom) throughout for $\lambda, \mu > 0$. In standard single-fluid FRW cosmology these two statements would be equivalent (via $\dot{H} = -3/2\,(1+\omega)H^2$); here they are **decoupled**, because $H(t)$ is prescribed independently of the fluid's equation of state in this reconstruction. The kinematic phantom divide ($q = -1$) and the thermodynamic phantom divide ($\omega = -1$) are both approached only asymptotically as $t \to \infty$, but from different sides and for different reasons.

4.7 $Om(z)$ Diagnostic

The $Om(z)$ diagnostic [28] is constructed purely from $H(z)$ and is constant, $Om(z) = \Omega_{m0}$, for ΛCDM in a flat, matter-dominated universe; departures from a horizontal line signal departure from ΛCDM. For a flat universe,

$$Om(z) = \frac{[H(z)/H_0]^2 - 1}{(1+z)^3 - 1}. \tag{38}$$

Using $a \propto \cosh^{\alpha/\beta}(\beta t)$ and $1 + z = a(t_0)/a(t)$, $H(z)$ is obtained by inverting $\cosh(\beta t) = \cosh(\beta t_0)(1+z)^{-\beta/\alpha}$ for $t(z)$ and evaluating $H\big(t(z)\big) = \alpha \tanh\big(\beta t(z)\big)$, where t_0 denotes a chosen reference ("present") epoch. Because $\cosh(\beta t) \geq 1$, this model's domain corresponds to $z \leq \cosh(\beta t_0)^{\alpha/\beta} - 1$; for the representative choice $t_0 = 2$ (for which $q_0 \equiv q(t_0) \approx -1.12$, consistent with $q(t) < -1$ throughout, §4.6), this gives $z \lesssim 3.1$.

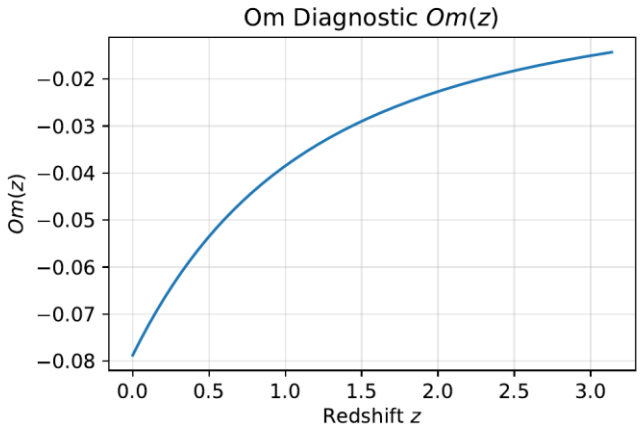

Fig.11: $Om(z)$ diagnostic (Eq. (38)) for the reference epoch $t_0 = 2$.

For $z \in [0, 2.7]$, $Om(z)$ is negative and slowly varying, $Om(z) \in [-0.078, -0.017]$, increasing (becoming less negative) with z (Fig. 11). A negative $Om(z)$ corresponds to an effective $\omega < -1$ *when interpreted within a single-fluid FRW template* – consistent with the kinematic $q(t) < -1$ found above – even though the genuine anisotropic-fluid $\omega(t) \geq -1$ (§4.2). This illustrates that $Om(z)$, like q, is a kinematic diagnostic and need not agree with the thermodynamic $\omega(t)$ of the true anisotropic source in a Bianchi I model; the mild slope of $Om(z)$ (rather than a horizontal line) indicates a persistent but small departure from ΛCDM across the redshift range probed.

5. CONCLUSIONS

We have presented an exact, anisotropic Bianchi type I cosmological model combining a power-law anisotropy ansatz $A = B^m$, $C = B^n$, a hyperbolic Hubble reconstruction $H(t) = \alpha \tanh(\beta t)$, and a cubic equation of state $p = \lambda\rho^3 + \mu\rho^2 - \rho$ for the effective cosmic fluid. The energy density (16), scale factor (11), expansion scalar, and shear scalar (28) are all regular for every finite $t \geq 0$, with no curvature singularities. The present solution should be viewed as an exact **late-time cosmological reconstruction** rather than a complete cosmological history: it is constructed to match a prescribed late-time $H(t)$ and does not aim to reproduce an earlier radiation- or matter-dominated epoch.

On the reconstruction philosophy: It is worth being explicit about the logic underlying this and similar exact solutions. Rather than specifying a dynamical fluid *a priori* and solving the field equations for the geometry it produces, we fix the geometry – via the power-law anisotropy ansatz $A = B^m$, $C = B^n$ and the hyperbolic parametrization (2) – and use the field

equations (5)–(8) to determine the stress-energy content $\rho(t), \omega(t), \gamma(t), \delta(t)$ *required* to support that geometry. The resulting fluid quantities are thus *derived, effective* descriptions consistent with the prescribed expansion history through Einstein's equations, rather than an independently specified source whose own dynamics generates $H(t)$ from some initial condition. This is the standard logic of $H(t)$- and equation-of-state reconstruction in cosmology, and for any geometry realizable by a physical fluid the two viewpoints are mathematically equivalent; it does mean, however, that the dynamical stability of $H(t)$ itself under small perturbations as opposed to the thermodynamic stability of the reconstructed fluid probed by $c_s^2(t)$ in §4.2 – lies outside the scope of the present analysis.

Kinematics: The model is everywhere accelerating, with $q(t) < -1$ for *all* $t > 0$ (diverging as $t \to 0^+$ and approaching -1 only as $t \to \infty$), and so describes a late-time/dark-energy-era phase rather than a complete cosmic history including an earlier decelerating epoch.

Anisotropy: The model is *exactly isotropic at* $t = 0$ ($\sigma^2(0) = 0$); both the shear scalar and the skewness parameters γ, δ grow from zero (or a removable singularity, in the case of γ, δ, caused by $\rho \to 0$) toward small, non-zero, permanent constants ($\sigma_\infty^2 \approx 0.0144$, $\gamma_\infty \approx -0.100$, $\delta_\infty \approx -0.201$). Most directly, the anisotropy ratio σ^2/θ^2 (Eq. (30)) is *exactly constant for all cosmic time* ($\approx 1/900$ for the adopted m, n), depending only on m, n. The universe therefore evolves toward a state of permanent, bounded (frozen) anisotropy rather than isotropizing; this residual anisotropy is controlled entirely by m, n (via α, β for the absolute normalization of σ^2, but $\gamma_\infty, \delta_\infty$ and σ^2/θ^2 depend only on m, n) and vanishes identically in the isotropic limit $m = n = 1$. Notably, $\gamma(t)$ and $\delta(t)$ are independent of the equation-of-state parameters λ, μ, being fixed purely by the geometry.

Observational context: We have not attempted a quantitative comparison of the frozen anisotropy level $\sigma^2/\theta^2 \approx 1.11 \times 10^{-3}$ with observational bounds on cosmic anisotropy (e.g. from Planck CMB temperature and polarization data, which typically constrain shear-type anisotropy to levels many orders of magnitude smaller than the illustrative value obtained here for $m = 1.1, n = 0.9$). The present work is intended as an exact theoretical solution demonstrating the existence and properties of a frozen-anisotropy late-time state within this class of models; $\sigma^2/\theta^2 = K/[3(m + n + 1)^2]$ can be made arbitrarily small by choosing m, n closer to unity, so the model is not in itself excluded, but a detailed confrontation with Planck (and other) anisotropy constraints – including the appropriate translation between this Bianchi I shear parameter and observational anisotropy estimators – is deferred to future work.

Effective fluid thermodynamics: The effective equation-of-state parameter $\omega(t)$ moves monotonically from the de Sitter value $\omega = -1$ at $t = 0$ to a mild quintessence value $\omega_\infty \approx -0.199$ at late times. The null energy condition is satisfied for all t; the strong energy condition is violated only in a brief early window ($t \lesssim 2.1$) and is restored thereafter. For $\lambda, \mu > 0$ as adopted here, phantom behaviour ($\omega < -1$) is never realized; it would require $\lambda < 0$ or $\mu < 0$.

Kinematic diagnostics: The jerk parameter $j(t) = 1 + k(3 - 2k)\,\mathrm{csch}^2(\beta t)$ ($k \equiv \beta/\alpha$) satisfies $j > 1$ for all t, decreasing monotonically from $j \to \infty$ as $t \to 0^+$ to $j \to 1$ as $t \to \infty$. The statefinder trajectory $(s, r) \equiv (s, j)$ approaches the ΛCDM fixed point $(0,1)$ from the quintessence-like quadrant $s < 0$, $r > 1$. The $Om(z)$ diagnostic, evaluated about a representative present epoch $t_0 = 2$, is negative and slowly varying, $Om(z) \in [-0.078, -0.017]$ for $z \in [0,2.7]$, signalling a mild but persistent departure from ΛCDM consistent with $q(t) < -1$. We note that the kinematic phantom-like behaviour ($q < -1$, $Om < 0$) coexists with the thermodynamically non-phantom $\omega(t) \geq -1$ – a decoupling possible only because $H(t)$ is prescribed independently of the fluid's equation of state in this anisotropic reconstruction (§4.6).

Causality: The sound-speed parameter $c_s^2(t)$ satisfies $c_s^2 \leq 1$ throughout for the adopted $(\lambda, \mu) = (0.02, 0.1)$, which satisfy the bound $3\lambda\rho_\infty^2 + 2\mu\rho_\infty \leq 2$ derived in §4.2. Parameter choices violating this bound (e.g. $\mu = 0.5$ with $\lambda = 0.02$, giving $c_s^2(\infty) \approx 4.4$) lead to a superluminal, acausal effective sound speed at late times and should be avoided, or the model's validity restricted to the time range where $c_s^2 \leq 1$.

In summary, the present work provides an exactly solvable Bianchi type I framework for a universe that begins in a state of perfect isotropy, passes through a transient, de Sitter-like, SEC-violating phase, and relaxes into a permanently but mildly anisotropic, causally consistent, quintessence-dominated late-time state – a scenario complementary to models that isotropize at late times, with all qualitative features controlled transparently by $(\alpha, \beta, m, n, \lambda, \mu)$ subject to the causality bound .

REFERENCES

[1] A. G. Riess et al., Astron. J. **116**, 1009 (1998).

[2] S. Perlmutter et al., Astrophys. J. **517**, 565 (1999).

[3] A. Einstein, Sitzungsber. Preuss. Akad. Wiss. Berlin, 142 (1917).

[4] G. F. R. Ellis and M. A. H. MacCallum, Commun. Math. Phys. **12**, 108 (1969).

[5] T. Padmanabhan, Phys. Rept. **380**, 235 (2003).

[6] E. J. Copeland, M. Sami and S. Tsujikawa, Int. J. Mod. Phys. **D15**, 1753 (2006).

[7] S. Nojiri and S. D. Odintsov, Phys. Rept. **505**, 59 (2011).

[8] R. R. Caldwell et al., Phys. Rev. Lett. **91**, 071301 (2003).

[9] M. Novello and S. E. P. Bergliaffa, Phys. Rept. **463**, 127 (2008).

[10] Y. F. Cai et al., Phys. Rept. **493**, 1 (2010).

[11] A. Friedmann, Z. Phys. **10**, 377 (1922).

[12] H. P. Robertson, Astrophys. J. **82**, 284 (1935).

[13] A. G. Walker, Proc. London Math. Soc. **42**, 90 (1937).

[14] S. Dodelson, *Modern Cosmology*, Academic Press (2003).

[15] V. Mukhanov, *Physical Foundations of Cosmology*, Cambridge University Press (2005).

[16] J. A. Peacock, *Cosmological Physics*, Cambridge University Press (1999).

[17] L. Amendola and S. Tsujikawa, *Dark Energy: Theory and Observations*, Cambridge University Press (2010).

[18] V. Sahni and A. Starobinsky, Int. J. Mod. Phys. **D9**, 373 (2000).

[19] V. Sahni et al., JETP Lett. **77**, 201 (2003).

[20] K. Bamba et al., Astrophys. Space Sci. **342**, 155 (2012).

[21] C. W. Misner, Astrophys. J. **151**, 431 (1968).

[22] K. C. Jacobs, Astrophys. J. **153**, 661 (1968).

[23] V. A. Belinskii and I. M. Khalatnikov, Sov. Phys. JETP **36**, 591 (1973).

[24] J. Wainwright and G. F. R. Ellis, *Dynamical Systems in Cosmology*, Cambridge University Press (1997).

[25] M. S. Berman, Nuovo Cimento **B74**, 182 (1983).

[26] D. R. K. Reddy et al., Astrophys. Space Sci. **357**, 6 (2015).

[27] V. Sahni, T. D. Saini, A. A. Starobinsky and U. Alam, JETP Lett. **77**, 201 (2003).

[28] V. Sahni, A. Shafieloo and A. A. Starobinsky, Phys. Rev. **D78**, 103502 (2008).